Fish & Shellfish Immunology 32 (2012) 816–827

Contents lists available at SciVerse ScienceDirect

Fish & Shellfish Immunology

journal homepage: www.elsevier.com/locate/fsi

RNA-seq analysis of mucosal immune responses reveals signatures of intestinal barrier disruption and pathogen entry following *Edwardsiella ictaluri* infection in channel catfish, *Ictalurus punctatus*

Chao Li [a], Yu Zhang [a], Ruijia Wang [a], Jianguo Lu [a], Samiran Nandi [b], Sriprakash Mohanty [b], Jeffery Terhune [a], Zhanjiang Liu [a], Eric Peatman [a,*]

[a] *The Fish Molecular Genetics and Biotechnology Laboratory, Department of Fisheries and Allied Aquacultures and Program of Cell and Molecular Biosciences, Aquatic Genomics Unit, Auburn University, Auburn, AL 36849, USA*
[b] *Central Institute of Freshwater Aquaculture, Kausalyanga, Bhubaneswar, Orissa 751002, India*

ARTICLE INFO

Article history:
Received 28 December 2011
Received in revised form
2 February 2012
Accepted 3 February 2012
Available online 17 February 2012

Keywords:
Channel catfish
RNA-seq
Intestine
Fish
Immune response

ABSTRACT

The mucosal surfaces of fish (gill, skin, gastrointestinal tract) are important sites of bacterial exposure and host defense mechanisms. In mammalian systems, the intestinal epithelium is well characterized as both a selectively permeable barrier regulated by junctional proteins and as a primary site of infection for a number of enteric pathogens including viruses, bacteria, and parasites. The causative bacterium of enteric septicemia of catfish, *Edwardsiella ictaluri*, is believed to gain entry through the intestinal epithelium, with previous research using a rat intestinal epithelial cell line (IEC-6) indicating actin polymerization and receptor-mediated endocytosis as potential mechanisms of uptake. Here, we utilized high-throughput RNA-seq to characterize the role of the intestinal epithelial barrier following *E. ictaluri* challenge. A total of 197.6 million reads were obtained and assembled into 176,481 contigs with an average length of 893.7 bp and N50 of 1676 bp. The assembled contigs contained 14,457 known unigenes, including 2719 genes not previously identified in other catfish transcriptome studies. Comparison of digital gene expression between challenged and control samples revealed 1633 differentially expressed genes at 3 h, 24 h, and 3 day following exposure. Gene pathway analysis of the differentially expressed gene set indicated the centrality of actin cytoskeletal polymerization/remodelling and junctional regulation in pathogen entry and subsequent inflammatory responses. The expression patterns of fifteen differentially expressed genes related to intestinal epithelial barrier dysfunction were validated by quantitative real-time RT-PCR (average correlation coeff. 0.92, $p < 0.001$). Our results set a foundation for future studies comparing mechanisms of pathogen entry and mucosal immunity across several important catfish pathogens including *E. ictaluri*, *Edwardsiellatarda*, *Flavobacterium columnare*, and virulent atypical *Aeromonas hydrophila*. Understanding of molecular mechanisms of pathogen entry during infection will provide insight into strategies for selection of resistant catfish brood stocks against various diseases.

1. Introduction

Mucosal surfaces form a thin physical barrier between the external environment and the internal milieu. This epithelial monolayer not only serves to mediate interactions between pathogen sensors and mucosa-associated lymphoid tissue (MALT) but also carries out other physiological roles such as nutrient absorption and waste secretion [1]. In mammalian systems, the intestinal mucosal epithelium is well characterized as both a selectively permeable barrier regulated by junctional proteins and as a primary site of infection for a number of enteric pathogens including viruses, bacteria, and parasites [2]. Intestinal diseases often lead to disruption or exploitation of barrier components either through co-opting them as receptors for attachment and internalization, through pathogen release of targeted effector molecules, or through stimulation of host inflammatory responses which ultimately compromise junctional integrity. Disruption of the apical junction complex (AJC), consisting of the tight junction, adherens junction, and desmosome, structurally impacts epithelial cell integrity via junctionally-linked actin filaments and disrupts

* Corresponding author. Tel.: +1 334 844 4085; fax: +1 334 844 9208.
E-mail address: peatmer@auburn.edu (E. Peatman).

1050-4648/$ – see front matter © 2012 Elsevier Ltd. All rights reserved.
doi:10.1016/j.fsi.2012.02.004

large cytoplasmic scaffolding proteins leading to dysregulated cell signaling and regulation [3].

The mucosal surfaces of fish (gills, skin, gastrointestinal tract) are also known as sites of pathogen exposure and are the focus of specific host defense mechanisms. Several studies have begun to examine the cellular and molecular composition of mucosal surfaces in salmonids [4–10], carp [11], cod [12] and flounder [13]. Farmed fish, like other vertebrates, are susceptible to a large number of pathogens with primary or secondary routes of entry through the gastrointestinal (GI) tract and which are capable of causing widespread mortality. Among these are *Aeromonas hydrophila*, *Aeromonas salmonicida*, *Mycobacterium marinum*, *Edwardsiella ictaluri*, *Edwardsiella tarda*, *Vibrio anguillarum*, and *Streptococcus iniae*. While our knowledge of cellular actors in teleost intestinal immunology has grown considerably [14], few studies have examined the molecular processes and pathways triggered following bacterial invasion and passage through the intestinal mucosa. Jima et al. [15] examined the transcriptional consequences of the lack of adaptive immunity (rag1−/−) in the zebrafish intestine, while Davey et al. [16] recently profiled gilthead sea bream intestinal responses to myxosporean parasite infection. Both studies utilized microarrays to examine expression levels of known transcripts.

Catfish (*Ictalurus* spp.), the dominant aquaculture species in the U.S., suffers from widespread disease outbreaks due to a number of enteric pathogens, including *A. hydrophila*, *E. tarda*, and *E. ictaluri*. The last of these, the Gram-negative, rod-shaped bacterium *E. ictaluri*, and its associated disease enteric septicemia of catfish (ESC), is commonly associated with widespread mortality through both acute and chronic infections in ponds. It has long been hypothesized that observed differences in disease susceptibility between catfish species and strains are due to the differing ability of the host to prevent pathogen attachment and entry at mucosal epithelial sites on the gill, skin, and gastrointestinal tract [17–19]. However, no studies have systematically studied the intestinal mucosal barrier and associated immune responses in this context. Hebert et al. [20] evaluated the composition of intestinal tract immune cells in channel catfish. Most relevant to this study, Skirpstunas and Baldwin [21] conducted invasion trials using *E. ictaluri* and mammalian, fish and harvested channel catfish enteric epithelial cells. They reported that pre-incubation of intestinal cell lines with cytochalasin D (microfilament depolymerizer) and monodansylcadaverine (blocks receptor-mediated endocytosis) reduced *E. ictaluri* invasion, indicating potential routes of entry. To begin to understand the elements of catfish mucosal immune responses, here we examined transcriptional profiles of the catfish intestine at three timepoints following experimental infection with *E. ictaluri*. Utilizing RNA-seq technology we captured 1633 differentially expressed genes with critical functional roles in cytoskeletal/muscle fiber dynamics, junctional modification, lysosome/phagosome regulation, immune activation and inflammation, attachment and pathogen recognition, and endocrine/growth disruption. Identification of the molecular actors in catfish mucosal immunity will advance our knowledge of teleost immunology and speed the development of targeted detection assays and therapeutants.

2. Methods

2.1. Experimental animals and tissue collection

All procedures involving the handling and treatment of fish used during this study were approved by the Auburn University Institutional Animal Care and Use Committee (AU-IACUC) prior to initiation. Marion channel catfish (average size 35 ± 1.3 g) were reared at the Auburn University Fish Genetics Research Unit prior to challenge. Challenges followed established detailed protocols for ESC [22] and [23]. Fish were challenged in 30 L (20 L water) aquaria with 3 control and 3 treatment groups. Aquaria were randomly divided into sampling timepoints-3 h treatment, 24 h treatment, 3 d treatment, 3 h control, 24 h control, and 3 d control with forty fish in each aquarium. The MS-S97-773 isolate of *E. ictaluri* bacteria was obtained from a natural outbreak and utilized in the experimental challenge. Bacteria were re-isolated from a single symptomatic fish and biochemically confirmed to be *E. ictaluri* using standard procedures. Briefly, isolates were streaked out on BHI agar and grown at 25 °C for 48 h and confirmed by appearance (small, punctate white colonies) and through biochemical assay (oxidase negative, fermentative in O/F glucose or glucose motility deeps (GMD), triple sugar iron (TSI) slant reaction K/A with no H_2S, and negative for indole production in tryptone broth). Following confirmation, the bacteria were inoculated into brain heart infusion (BHI) broth and incubated in a shaker (180 rpm) incubator at 25 °C overnight. The concentration of the bacteria was determined using colony forming unit (CFU) per mL by plating 10 μl of 10-fold serial dilutions onto BHI agar plates. During challenge, 200 mL bacterial culture with a concentration of 4×10^8 CFU/ml was added into the aquaria. Water was turned off in the aquaria for 2 h of immersion exposure, and then continuous water flow-through resumed for the duration of the challenge experiment.

At 3 h, 24 h and 3 d after challenge, 30 fish were collected from each of the appropriate control and treatment aquaria at each timepoint and euthanized with MS-222 (300 mg/L) buffered with sodium bicarbonate. The entire intestinal tracts from 10 fish were dissected, bisected and gently washed with cold, sterile PBS and pooled together in RNAlater. Samples were stored at 4 °C overnight following collection and then transferred to −80 °C prior to RNA extraction. During the challenge, symptomatic treatment fish and control fish were collected and confirmed to be infected with *E. ictaluri* and pathogen-free, respectively, at the Fish Disease Diagnostic Laboratory, Auburn University.

2.2. RNA extraction, library construction and sequencing

Prior to RNA extraction, samples were removed from the −80 °C freezer and ground with sterilized mortar and pestle in the presence of liquid nitrogen to a fine powder. Total RNA was extracted from tissue powder using the RNeasy Plus Kit (Qiagen) following manufacturer's instructions and treated with RNase free DNase I (Qiagen) to remove genomic DNA. RNA concentration and integrity of each sample was measured on an Agilent 2100 Bioanalyzer using a RNA Nano Bioanalysis chip. For each timepoint, equal amounts of RNA from the three treatment replicates were pooled for RNA-seq library construction. For the control samples, the replicate pools spanned each of the three timepoints (0 h, 24 h, and 3 d). A master pool composed of equal amounts of each replicate control pool was formed for use in RNA-seq.

RNA-seq library preparation and sequencing was carried out by HudsonAlpha Genomic Services Lab (Huntsville, AL, USA). cDNA libraries were prepared with 2.14–3.25 ug of starting total RNA and using the Illumina TruSeq RNA Sample Preparation Kit (Illumina), as dictated by the TruSeq protocol. The libraries were amplified with 15 cycles of PCR and contained TruSeq indexes within the adapters, specifically indexes 1–4. Finally, amplified library yields were 30 ul of 19.8–21.4 ng/ul with an average length of ~270 bp, indicating a concentration of 110–140 nM. After KAPA quantitation and dilution, the libraries were clustered 4 per lane and sequenced on an Illumina HiSeq 2000 instrument with 100 bp paired end (PE) reads.

2.3. De novo assembly of sequencing reads

Before assembly, raw reads were trimmed by removing adapter sequences and ambiguous nucleotides. Reads with quality scores less than 20 and length below 30 bp were all trimmed. The resulting high-quality sequences were used in subsequent assembly.

The *de novo* assembly was performed by various de Brujin graph assemblers to obtain the best assembly results [24]. Briefly, the clean reads were first hashed according to a predefined k-mer length, the 'k-mers'. After capturing overlaps of length k−1 between these k-mers, the short reads were assembled into contigs. We used publicly available programs ABySS version 1.2.5 [25] and Trans-ABySS version 1.2.0, Velvet version 1.1.04 [26] and Assembly Assembler version 1.3, and commercially available CLC Genomics Workbench version 4.7.2.

The clean reads from all timepoints were used as input in all the assemblers. ABySS and Velvet assemblies were performed at various k-mer lengths. In ABySS, the k-mer size was set from 50 to 96, assemblies from all k-mers were merged into one assembly by Trans-ABySS. In Velvet, the k-mer was equal to 50, 55, 61, 67, 75, 85 and 97 with insert length 268, and AssemblyAssembler version 1.3 was used to merge different assemblies. In CLC Genomics Workbench, the assembly was performed using default settings. In order to reduce redundancy, the assembly results from different assemblers were passed to CD-Hit [27] version 4.5.4 and CAP3 [28] for multiple alignment and consensus building after trimming contigs less than 200 bp. The threshold was set as identity equal to 1 in CD-Hit, the minimal overlap length and identity equal to 100 bp and 99% in CAP3.

2.4. Gene annotation and ontology

Following selection of the Trans-ABySS assembly based on contig number and contig length, assembly contigs were used as queries against the NCBI zebrafish protein database, the UniProtKB/SwissProt database and the non-redundant (nr) protein database using the BLASTX program. The cutoff E-value was set at 1e-5 and only the top gene id and name were initially assigned to each contig. Gene ontology (GO) annotation analysis was performed using the zebrafish BLAST results in Blast2GO version 2.5.0 [29], which is an automated tool for the assignment of gene ontology terms. The zebrafish BLAST result or the nr BLAST result (when a "hypothetical" result was returned in the zebrafish database), was imported to BLAST2GO. The final annotation file was produced after gene ID mapping, GO term assignment, annotation augmentation and generic GO-Slim process. The annotation result was categorized with respect to Biological Process, Molecular Function, and Cellular Component at level 2.

2.5. Identification of differentially expressed contigs

The high-quality reads from each sample were mapped onto the Trans-ABySS reference assembly using CLC Genomics Workbench software. During mapping, at least 95% of the bases were required to align to the reference and a maximum of two mismatches were allowed. The total mapped reads number for each transcript was determined, and then normalized to detect RPKM (Reads Per Kilobase of exon model per Million mapped reads). The proportions-based test was used to identify the differently expressed genes between control and 3 h, 24 h and 3 d with p-value <0.05. The proportions-based test method, which was originally developed for SAGE data, allows an estimation of differential expression based on single measurements of tag/read counts for two conditions [30]. After quantile normalization of the RPKM values, fold changes were calculated. Analysis was performed using the RNA-seq module and the expression analysis module in CLC Genomics Workbench. Transcripts with absolute fold change values of larger than 1.5 and total read number larger than 5 were included in analysis as differently expressed genes.

Contigs with previously identified gene matches were carried forward for further analysis. Functional groups and pathways encompassing the differently expressed genes were identified based on GO analysis, pathway analysis based on the Kyoto Encyclopedia of Genes and Genomes (KEGG) database, and manual literature review.

2.6. Gene ontology and enrichment analysis

In order to identify overrepresented GO annotations in the differentially expressed gene set compared to the broader reference assembly, GO analysis and enrichment analysis of significantly expressed GO terms was performed using Ontologizer 2.0 [31] using the Parent-Child-Intersection method with a Benjammini-Hochberg multiple testing correction [32]. GO terms for each gene were obtained by utilizing zebrafish annotations for the unigene set. The difference of the frequency of assignment of gene ontology terms in the differentially expressed genes sets were compared to the overall catfish reference assembly. The threshold was set as FDR value <0.1.

2.7. Experimental validation – QPCR

Fifteen significantly expressed genes were selected for validation using real-time QPCR with gene specific primers designed using Primer3 software. Total RNA was extracted using the RNeasy Plus kit (Qiagen) following manufacturer's instructions and treated with RNase free DNase I (Qiagen) to remove genomic DNA. First strand cDNA was synthesized by iScript™ cDNA Synthesis Kit (Bio-Rad) according to manufacturer's protocol. All the cDNA products were diluted to 250 ng/μl and utilized for the quantitative real-time PCR reaction using the SsoFast™ EvaGreen® Supermix on a CFX96 real-time PCR Detection System (Bio-Rad Laboratories, Hercules, CA). The thermal cycling profile consisted of an initial denaturation at 95 °C (for 30 s), followed by 40 cycles of denaturation at 94 °C (5 s), an appropriate annealing/extension temperature (58 °C, 5 s). An additional temperature ramping step was utilized to produce melting-curves of the reaction from 65 °C to 95 °C. The housekeeping gene 18S was set as the reference gene, relative fold changes were calculated in the Relative Expression Software Tool version 2009 [33] based on the cycle threshold (Ct) values generated by q-RT-PCR. The triplicate fluorescence intensities of the control and treatment products for each gene, as measured by crossing-point values, were compared and converted to fold differences by the relative quantification method and assuming 100% efficiencies. Expression differences between control and treatment groups were assessed for statistical significance using a randomization test in the REST software. The mRNA expression levels of all samples were normalized to the levels of 18S ribosomal RNA gene in the same samples. Expression levels of 18S were constant between all samples (<0.30 change in Ct). A no-template control was run on all plates.

3. Results

3.1. ESC challenge

The artificial challenge with virulent *E. ictaluri* resulted in widespread mortality of infected fish at day 7 after exposure. No control fish manifested symptoms of ESC, and randomly selected

control fish were confirmed to be negative for *E. ictaluri* by standard diagnosis procedures (see Methods). Dying fish manifested behavior and external signs associated with ESC infection including hanging in the water column with head up and tail down and petechial hemorrhages along their ventral surface. *E. ictaluri* bacteria were successfully isolated from randomly selected treatment fish.

3.2. Sequencing of short expressed reads from catfish intestine

Illumina-based RNA-sequencing (RNA-seq) was carried out on intestine samples from control catfish as well as from those experimentally-challenged with *E. ictaluri* (3 h, 24 h and 3 d groups). Reads from timepoint-specific samples were distinguished through the use of multiple identifier (MID) tags. A total of 197.6 million 100 bp PE reads were generated on an Illumina HiSeq 2000 instrument in a single lane. Greater than 44 million reads were sequenced for each of the four libraries. After removing ambiguous nucleotides, low-quality sequences (quality scores <20) and sequences less than 30 bp, 99.19% (196 million) of the short reads were preserved (Supplementary Table 1). Raw read data are archived at the NCBI Sequence Read Archive (SRA) under Accession **SRP009069**.

3.3. De novo assembly of catfish intestinal transcriptome

Several differing sequence contig assembly algorithms and software programs recently have been developed to address assembly of RNA-seq reads [34]. Given the importance of assembly of long, accurate contigs to capture catfish genes and to correctly identify differential expression, we compared three prominent options for *de novo* transcriptome assembly as follows: Trans-ABySS, Velvet, and CLC Genomics Workbench (CLC). Among the three, CLC Genomics Workbench differs as commercial software with the ability to operate through a graphic–user interface (GUI) versus a Linux-based command–line interface for Velvet and Trans-ABySS.

3.3.1. Trans-ABySS

Forty-seven multiple k-mer (k-mer sizes 50–96) assemblies were performed in ABySS, and 15 million contigs were generated in total. Assemblies ranged from 44,663 contigs to 321,992 contigs with N50 sizes from 531 bp to 1453 bp. The combined assembly utilizing Trans-ABySS generated 630,209 contigs with average length of 725 bp and N50 size of 1676 bp (Table 1). The Trans-ABySS assembly contained 59.7% contigs longer than 200 bp, and 22.3% of contigs were longer than 1000 bp. Contigs less than 200 bp were removed from further analysis. Multiple-k algorithms produce redundant assemblies which may cause errors in subsequent analyses. Despite Trans-ABySS having its own built-in redundancy elimination solutions, we found that additional steps were required to identify a unique reference. Approximately 0.5 million contigs were removed during the length and redundancy filtration steps (CD-Hit and CAP3), resulting in a final average contig size and contig number of 893.7 bp and 176,481, respectively (Table 1).

3.3.2. Velvet

Seven assemblies (seven k-mers between 50 and 99 bp) were generated in Velvet totaling 1.2 million contigs. Velvet's AssemblyAssembler was utilized to obtain the combined assembly, resulting in 186,451 contigs with average length of 500.8 bp and N50 of 1508 bp. Contig length distributions were distinct from the assembly from Trans-ABySS – 69.2% of contigs were longer than 200 bp but only 11.2% of contigs were longer than 1000 bp. The average contig size and contig numbers were increased to 743 bp and reduced to 67,081, respectively, after stand-alone redundancy filtration (CD-Hit and CAP3) using conservative cutoff parameters (Table 1).

Table 1
Summary of *de novo* assembly results of Illumina sequence data from catfish intestine using various assemblers.

	Trans-ABySS	Velvet	CLC
Contigs(≥100 bp)	630,209	186,451	332,383
Large contigs (≥1000 bp)	140,357	20,881	20,431
Maximum length (bp)	17,585	16,860	17,653
Average length (bp)	725.1	500.8	339.0
N50 (bp)	1676	1508	611
Contigs after length filtering (≥200 bp)	376,005	129,025	120,534
Percentage contigs kept after length filtering	59.66%	69.20%	36.26%
Average contig length after length filtering (bp)	1120	653.7	691.2
Contigs (After CD-HIT-EST+ CAP3)	176,481	67,081	120,534
Average length (bp) (After CD-HIT-EST+ CAP3)	893.7	743.0	691.2
Reads mapped to final reference (%)	88.42%	54.26%	38.88%

3.3.3. CLC Genomics Workbench

A fast single k-mer length (k = 24; automatically selected) assembly was performed by CLC Genomics Workbench resulting in 332,383 contigs with average length 339 bp and N50 size 611 bp (Table 1). Only 36.3% of contigs were longer than 200 bp and 6.15% of contigs were longer than 1000 bp. Due to the non-redundant single-k approach, no changes resulted following CD-Hit/CAP-3 filtering.

3.3.4. Best assembly selection

In a comparison of the assemblies among the three different approaches (Table 1), Trans-ABySS consistently generated a larger percentage of large contigs, the longest final contig size, and the largest number of contigs after filtering. Additionally, a total of 88.42% of the initial reads mapped to the final Trans-ABySS reference assembly, compared to 54.26% in Velvet and 38.88% in CLC, illustrating the more comprehensive nature of the Trans-ABySS assembly. Therefore, the Trans-ABySS assembly was selected for subsequent gene discovery and differential expression analysis. Assembled contig sequences are available upon request.

3.4. Gene identification and annotation

BLAST-based gene identification was performed to annotate the channel catfish transcriptome and inform downstream differential expression analysis. After gene annotation, 73,330 (41.55%) of the Trans-ABySS contigs had a significant BLAST hit against 15,640 unique zebrafish genes (unigenes; Table 2). In order to further evaluate the quality of the assembled genes, 14,457 unigenes were identified based on hits to the zebrafish database with the more stringent criteria of a BLAST score ≥100 and E-value ≤1e−20 (quality matches). Among these quality unigene matches, 2719 represented genes which had not been previously captured by previous EST and general RNA-seq transcriptome work in catfish [35,36]. The same BLAST criteria were used in comparison of the Trans-ABySS reference contigs with the UniProt and nr databases. The largest number of matches was to the nr database with 77,577 contigs with putative gene matches to nr and 19,960 quality unigene matches (Table 2).

Unique gene-coding contigs from the channel catfish reference assembly were then used as inputs to perform gene ontology (GO)

Table 2
Summary of gene identification and annotation of assembled catfish contigs based on BLAST homology searches against various protein databases (Zebrafish, UniProt, nr). Putative gene matches were at E-value ≤1e−-5. Hypothetical gene matches denote those BLAST hits with uninformative annotation. Quality unigene hits denote more stringent parameters, including score ≥100, E-value ≤ 1e-20.

	Contigs with putative gene matches	Annotated contigs ≥500 bp	Annotated contigs ≥1000 bp	Unigene matches	Hypothetical gene matches	Quality unigene matches
Zebrafish	73,330	37,500	14,868	15,640	1154	14,457
UniProt	55,551	42,524	31,136	17,476	0	15,786
NR	77,577	51,215	34,742	23,205	2130	19,960

annotation by Blast2GO [29]. A total of 21,877 GO terms including 5448 (29.9%) cellular process terms, 6596 (30.15%) molecular functions terms and 9833 (44.95%) biological process terms were assigned to 14,457 unique gene matches. The percentages of annotated catfish sequences assigned to GO terms are shown in Supplementary Fig. 1. Analysis of level 2 GO term distribution showed that metabolic process (GO:0008152), cellular process (GO:0009987), binding (GO:0005488) and cell (GO:0005623) were the most common annotation terms in the three GO categories (Supplementary Fig. 1).

3.5. Identification and analysis of differentially expressed genes

A total of 4414 of the 176,481 (2.50%) final reference contigs showed significant differential expression for at least one timepoint following infection. Differentially expressed contigs had an average consensus length of 1088.5 bp. The identified contigs represented 1633 unigenes, including 1474 unique genes with more stringent criteria of a BLAST score ≥100 and E-value ≤1e−20, and 159 unique genes with BLAST E-value from 1e-20 to 1e-5 (Supplementary Table 2). In detail, there were 693 genes differentially expressed at 3 h after challenge relative to control, 918 genes differently expressed at 24 h after challenge relative to control, and 1035 genes differently expressed at 3 d after challenge relative to control (Table 3). Similar numbers of genes were up-regulated and down-regulated at 3 h and 24 h, with the largest number of genes (607) down-regulated at 3 d. Read coverage (average contig size) within the differentially expressed contigs ranged from 256 reads/contig at 3 d to 365 reads/contig at 3 h.

3.6. Enrichment and pathway analysis

The differently expressed unique genes were then used as inputs to perform gene ontology (GO) annotation by Blast2GO (Supplementary Fig. 2). Parent-child GO term enrichment analysis was performed for the 1633 unigenes to detect significantly over-represented GO terms. A total of 49 terms with p-value (FDR-corrected) < 0.1 were considered significantly overrepresented. Ten higher level GO terms were retained as informative for further pathway analysis (Supplementary Table 3). The GO terms include functions and processes including response to chemical stimulus, MHC protein complex, antigen processing and presentation, intermediate filament cytoskeleton, and antioxidant activity.

Table 3
Statistics of differently expressed genes at different timepoints following ESC challenge. Values indicate contigs/genes passing cutoff values of fold change ≥1.5 ($p < 0.05$) and read number per contig ≥5. Average contig size refers to reads/contig.

	3 h	24 h	3 d
Up-regulated	319	469	428
Down-regulated	374	449	607
Total	693	918	1035
Average contig size	365	285	256
Total unigenes	1633		

GO term analysis and downstream pathway analysis were complicated by the incomplete annotation and unique nomenclature characteristic of zebrafish proteins. Automated pathway analysis software often could not resolve zebrafish annotations into large functional categories or pathways. We used a combination of KEGG pathway analysis, manual re-annotation based on the nr database, and manual literature searches to identify six broad functional categories of genes observed to be differentially expressed in the catfish intestine following infection with an enteric pathogen, *E. ictaluri*. These categories are illustrated in the context of a representative diagram of the intestinal mucosal barrier (Fig. 1) and include: 1) cytoskeletal and muscle fiber dynamics; 2) junctional modification and disruption; 3) lysosome/phagosome-associated responses; 4) immune activation and inflammation; 5) attachment and pathogen recognition; and 6) endocrine/growth disruption. Table 4 lists key, non-redundant gene components of these categories. Putative functional roles and interactions of the genes in the context of *E. ictaluri* invasion and replication are discussed in detail below (Discussion).

3.7. Validation of RNA-seq profiles by QPCR

In order to validate the differentially expressed genes identified by RNA-Seq, we selected 15 genes for QPCR confirmation, selecting from those with differing expression patterns and from genes of interest based on functional enrichment and pathway results. DNase I-treated, column-purified total RNA samples from control, and 3 h, 24 h and 3 d following challenge (3 replicate sample pools ($n = 10$ for each pool)) were used for QPCR. Primers were designed based on contig sequences (Supplementary Table 4). Melting-curve analysis revealed a single product for all tested genes. Fold changes from QPCR were compared with the RNA-seq expression analysis results. As shown in Fig. 2, QPCR results were significantly correlated with the RNA-seq results at each timepoint (correlation coefficients 0.86–0.95, p-value <0.001). Values for the QPCR and RNA-seq results are given in Supplementary Table 5. In general, the RNA-seq results were confirmed by the QPCR results, indicating the reliability and accuracy of the Trans-ABySS reference assembly and RNA-seq expression analysis.

4. Discussion

Invasive pathogenic bacteria use a multitude of different strategies to penetrate host cells and evade killing. While these mechanisms have been the intense focus of microbiologists for decades, only recently have tools been developed to allow the capture of molecular signatures related to host responses and host-pathogen interactions during infection. Here we have utilized RNA-seq-based expression profiling to examine the transcriptional responses of channel catfish intestinal cells following experimental challenge with *E. ictaluri*, a Gram-negative bacterium.

The present work represents, to our best knowledge, the first RNA-seq-based expression study in catfish and one of a small, but growing, handful in fish species [e.g [37,38]. It is, therefore, of

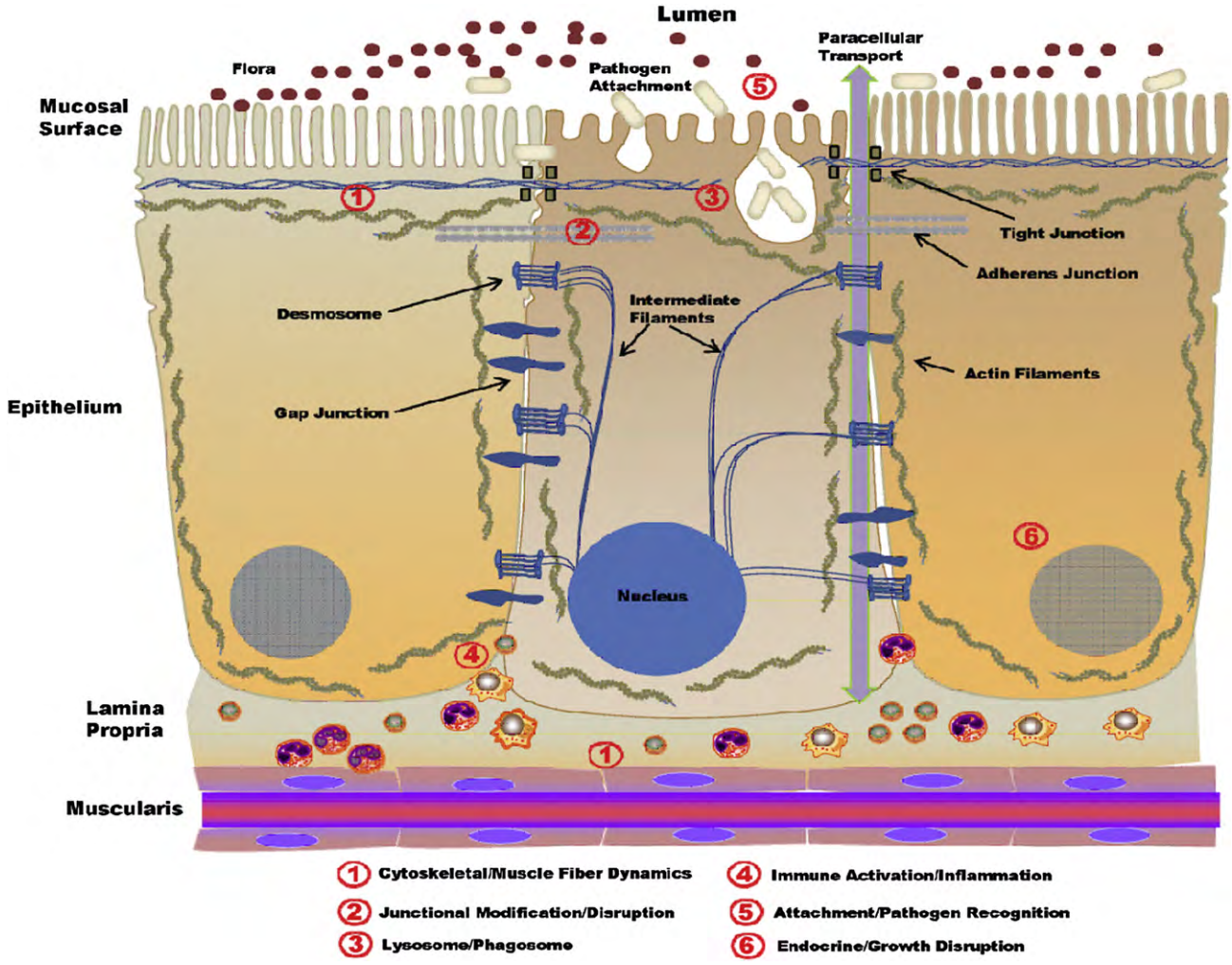

Fig. 1. Diagram of intestinal mucosal barrier structures and components putative functional categories of catfish responses to *E. ictaluri* infection are noted with circled numbers (1–6) referring to the accompanying legend.

interest to evaluate the suitability of sequence-based transcript quantification versus established standards such as real-time PCR and microarrays. In catfish, we previously used both a 19K [39] and a 28K microarray [22,40] to analyze changes in gene expression after perturbations of the immune system either from LPS injection or ESC challenge. These studies captured relatively small gene sets (e.g. 76 significant genes in blue catfish liver, [22]) in comparison with the 1633 unique differentially expressed genes reported here. This could reflect, in part, the ability of RNA-seq to quantify expression levels of novel transcripts. Trans-ABySS-based assembly of our Illumina sequence reads resulted in 176,481 contigs with average length of 893.7 bp. These contigs represented as many as 23,205 unique genes based on BLAST identity (Table 2), including 2719 genes previously missed in EST sequencing. These results match up well in comparison with previous extensive EST sequencing in multiple tissues from channel catfish and blue catfish which resulted in 14,776 unique genes from 111,578 contigs of average length of 771.3 bp [35].

Additional validation of RNA-seq methods for gene expression analysis was gained through QPCR analysis of expression of selected genes in each of the three timepoints. Transcripts with a variety of expression patterns in the RNA-seq results were tested. Overall, there was significant correlation between the two methods with coefficients ranging from 0.86 to 0.95, p-value <0.001 (Fig. 2). There was no consistent bias in expression level observed for either method (i.e. degree of fold change was not correlated with method). Additionally, a single product was amplified with all tested primer pairs, providing evidence that the contig assembly was accurate and did not result in chimeric transcripts. The QPCR validation also was an important indication that the master pooled samples (3 pools of 10 fish each) used for RNA-seq analysis reflected expression levels in the individual pools. While pooling samples obviously could have masked individual variation, our goal in the present study was to gain a broad understanding of catfish intestinal gene responses to infection and to provide early insights into important pathways and processes. Follow-up studies in our lab (either planned or underway) will use our results here as a foundation for more targeted studies comparing mucosal immune responses between susceptible and resistant lines of catfish, comparing mucosal immune responses to several enteric pathogens, and comparing immune responses to pathogens with those to associated vaccines.

Our study also represents the first characterization of the catfish intestinal transcriptome following infection and is, arguably, among the most comprehensive analyses of intestinal gene expression in teleost fish. The heterogeneous nature of the intestine, with mucosal epithelium, lamina propria, migrating leukocytes, and muscularis (Fig. 1), is additionally complicated by the

Table 4
Key channel catfish genes differentially expressed following ESC challenge. Bold values indicate timepoints where the gene was significantly changed relative to the control.

Functional classification	Gene name	Contig ID	3 h fold change	24 h fold change	3d fold change
Cytoskeletal/Muscle Fiber Dynamics	14-3-3 protein epsilon	Contig19138	**6.92**	2.13	2.33
	Actin, cytoplasmic 1	Contig5287	**−6.03**	−1.49	**2.09**
	AHNAK nucleoprotein	Contig22801	**7.27**	**9.02**	**8.73**
	Alpha-actin-1	Contig5133	**−21.4**	**−18.67**	**−20.74**
	Annexin A2	k66_684752	**−5.99**	−1.03	−2.34
	Annexin A2-like	Contig24251	−1.74	**−2.19**	**−3.86**
	Arp2/3	Contig17702	−1.62	**−1.98**	**−2.17**
	Basigin	Contig3778	**3.22**	**4.98**	**2.9**
	Calmodulin 1a	Contig10653	**3.12**	**2.55**	**2.3**
	CDC42SE2	Contig11032	**−5.54**	−1.37	−1.22
	Cofilin 2, like	Contig25509	−1.17	−1.5	**−1.81**
	Collagen alpha-1(V) chain	k_90380157	3.36	**4.81**	4.09
	EMILIN-1	Contig16606	**2.78**	**4.91**	**4.92**
	Epiplakin-like	Contig13325	3.04	**5.85**	**4.46**
	Ezrin like	Contig20491	1.21	**−4.2**	**−2.76**
	Filamin A, alpha	Contig476	**1.98**	**2.18**	**2.31**
	Gelsolin-like (CAPG)	k70_862348	**6.93**	**5.78**	**7.3**
	Keratin, type I cytoskeletal 13	Contig10499	**−11.31**	**−4.43**	**−7.34**
	LIMA1	Contig38617	**3.86**	**4.76**	**3.44**
	Myosin heavy chain	Contig14966	**−72.4**	**−21.66**	**−43.6**
	Myosin light chain kinase b	Contig24474	**1.51**	**1.46**	**1.47**
	Myosin regulatory light polypeptide 9	Contig42338	**3.01**	**6.47**	**7.45**
	Myosin, light polypeptide 3	Contig10157	**−6.2**	**−8.78**	**−4.31**
	Myosin-VII	Contig6265	**2.02**	**2.55**	**2.11**
	Paxillin	Contig11500	1.61	**2.23**	**2.19**
	Profilin-2	Contig16251	−1.06	**−2.37**	1.12
	Protocadherin 1-like	Contig20123	2.01	**2.65**	2.07
	Ras-related protein R-Ras	Contig15983	**4.2**	2.86	**3.85**
	Small GTPase RhoA	Contig4251	−1.43	**−1.73**	**−3.23**
	Supervillin-like, partial	Contig12472	**4.82**	2.9	**4.18**
	Synaptopodin-2	Contig17899	1.95	**2.37**	**2.96**
	Tropomyosin alpha-3 chain 2	k76_731419	**−4.65**	**−3.37**	−1.15
	Type I cytokeratin, enveloping layer	Contig38426	2.49	1.2	**5.96**
Junctional Modification/ Disruption	Aquaporin 8	Contig14861	1.35	**3.02**	**6.42**
	Cadherin 1, type 1 preproprotein	Contig34588	2.01	**3.12**	**4.57**
	Claudin 15a	k65_774609	**−3.28**	**−3.09**	−1.26
	Claudin-9	Contig16617	**−2.31**	−1.24	−1.11
	Desmocollin 2	Contig26678	**3.39**	**3.47**	**3.67**
	Desmoglein-2	Contig6653	2.18	**2.83**	1.95
	Desmoplakin	Contig14264	1.62	**2.16**	**2.36**
	Epithelial cadherin precursor	Contig38947	**−2.75**	−1.22	**−6.04**
	MAGI3	Contig3167	2.76	**5.13**	2.75
	Occludin-like	Contig1340	1.48	**1.86**	1.32
	Plakophilin 3	Contig27202	**1.45**	**1.6**	1.38
	Zonadhesin-like	Contig19706	**2.39**	**1.3**	**1.59**
Lysosome/Phagosome	ADP-ribosylation factor 1	Contig6638	**2.7**	1.75	1.56
	Beta-galactosidase	k51_958092	**2.06**	**−2.87**	−1.46
	Cathepsin Z	Contig3027	**9.78**	**6.36**	**15.49**
	CD63 antigen	Contig39977	**3.34**	**2.22**	1.51
	Cytoplasmic dynein 1 heavy chain 1	Contig5492	2.28	2.54	**4.73**
	ER aminopeptidase 2	Contig23351	−1.01	1.42	**3.94**
	Glucocerebrosidase-like	k_87479012	1.41	**2.87**	1.83
	Hexosaminidase B	k_92109136u	−1.04	**−3.29**	**−5.5**
	Immunoglobulin heavy mu-like	Contig31220	−1.38	**−3.68**	**−2.89**
	Legumain	Contig15202	**1.71**	**−1.27**	**1.58**
	Lysosomal alpha-mannosidase	Contig19918	**1.69**	**−1.43**	1.23
	Lysosomal membrane glycoprotein 2	Contig18023	**2.95**	2.21	1.01
	Lysosomal protective protein	Contig3023	**2.21**	**1.58**	**1.53**
	Lysosomal transmembrane protein 4A	Contig996	−1.33	**2.31**	1.59
	Lysosome glycoprotein 1 isoform 2	Contig16856	−1.24	**−1.57**	−1.03
	Lysozyme G-like 1	Contig26961	−1.33	−1.39	**2.44**
	Lysozyme-like protein 2	Contig39554	**−2.75**	−2.41	**7.36**
	MHC class I UXA2	Contig29433	**−12.4**	**−2.52**	−1.14
	MHC class I ZE like	Contig33016	**3.79**	**10.1**	**5.59**
	MHC class II alpha chain 1	Contig35822	**−8.39**	**−20.92**	**−9.48**
	MHC class II beta	Contig23428	**−4.56**	**−6.92**	**−3.88**
	NADPH oxidase 1	Contig38009	**−2.98**	**−4.55**	**−3.21**
	NOXO1	Contig4675	**−2.68**	**−7.35**	**−6.47**
	Pip5k1b	k51_308390	2.22	2.86	**6.87**
	Prosaposin	Contig10452	1.49	1.08	**1.63**
	Sialidase-1	k50_918038	**4.58**	2.76	**4.33**
	Sphingosine–phosphate phosphotase 2	k58_866656	−3.39	−1.48	**−5.01**
	Thrombospondin 1	k52_945196	2.83	**3.82**	**3.97**
	Transport protein Sec61 alpha-like 1	k56_745918u	**−2.98**	−1.45	−1.59

Table 4 (*continued*)

Functional classification	Gene name	Contig ID	3 h fold change	24 h fold change	3d fold change
Immune Activation/ Inflammation	Apolipoprotein B	Contig5210	**3.16**	**3.36**	**2.05**
	C1Q subcomponent-binding protein	k66_875137	**−9.95**	−1.81	−1.45
	C1q-like 3	k66_929422	**−4.34**	−1.97	−2.79
	CC chemokine 25-like	Contig43069	**−2.43**	−1.47	**1.65**
	CC chemokine SCYA102	Contig10839	1.37	**−3.27**	−1.28
	CC chemokine SCYA104-like	Contig37889	1.02	**−4.19**	**−3.8**
	CC chemokine SCYA113	Contig1891	**−1.87**	**−2.63**	**1.39**
	CC chemokine SCYA117-like	Contig29792	1.52	**4.83**	2.05
	CC chemokine SCYA124	k64_453703u	−1.6	**2.79**	2.39
	CD209 antigen (DC-SIGN)	Contig3473	−1.64	**−2.84**	**−2.43**
	Chemokine CXCL12	Contig160	**2.55**	**2.51**	**2.41**
	Chemokine CXCL2	Contig22481	1.23	1.45	**3.53**
	Chemokine receptor-like 1-like	Contig4932	1.98	2.55	**3.21**
	Complement C4-1-like	Contig1264	**3.46**	1.68	−1.18
	Complement C6	Contig11023	1.23	1.23	**5.03**
	Complement C7	Contig17426	−2.62	−1.31	**2.99**
	Glutathione peroxidase 3	Contig16143	**−3.8**	**−3.74**	**−6.59**
	Hypermethylated in cancer 1 protein	k66_275227	**4.79**	**5.76**	3.83
	IgGFc-binding protein	k61_673619	**4**	**2.41**	**2.13**
	Interleukin 11 receptor, alpha	Contig853	**2.42**	**2.81**	**2.3**
	Interleukin 7 receptor	Contig26716	1.87	**3.79**	2.29
	Jun D proto-oncogene-like	k70_513305	**6.6**	**4.59**	2.3
	LEAP-2	Contig14731	**−2.1**	**−2.3**	−1.44
	Macrophage MIF	Contig40086	**3.96**	**9.6**	**4.4**
	Metallothionein-2	Contig38077	**−1.81**	**−1.54**	**−3.04**
	Microfibrillar-associated protein 4-like	Contig40286	1.59	1.04	**2.79**
	MMP9	Contig9368	−2.14	**−3.98**	−2.15
	MMP13	k54_922997	**−3.02**	**−5.91**	**−8.39**
	Neurotoxin/C59/Ly-6-like protein	k71_580318	**−1.58**	**−3.86**	**−5.96**
	NF-kappa-B p100 subunit	Contig2282	2.61	2.2	**3.71**
	Novel immune-type receptor 6a	Contig39942	**−2.07**	−1.71	**−2.18**
	Novel immune-type receptor 7	Contig39943	**4.17**	**3.83**	**4.56**
	Prostaglandin E synthase 3	k50_966012u	**5.18**	**5.39**	**4**
	Serum amyloid P component-like 2	Contig32897	**−3.07**	**−2.42**	**−3.42**
	Sialoadhesin	Contig10481	3.57	2.03	**8.5**
	Suppressor of cytokine signaling 1	Contig38899	**3.08**	**−1.95**	**−1.85**
	T-cell receptor beta C beta region	k66_937487	1.17	**4.33**	1.22
	TNF receptor superfamily, member 1a	k78_684621	**7.09**	4.71	**7.89**
	Tnf receptor-associated factor 2b 1	Contig5463	**2.43**	1.05	1.15
	Tumor protein p53-inducible protein 1	Contig15021	1.7	**−10.06**	**−5.06**
Attachment/Pathogen Recognition	Fibronectin 1b-like 1	Contig8744	4.22	5.08	**8.75**
	Integrin, alpha-3a	Contig4954	2.19	**3.25**	**2.68**
	Integrin, beta 1b	k50_930983	**2.19**	**2.17**	**2.32**
	Integrin, beta 4	Contig1086	1.75	**2.19**	**2.43**
	Mucin 2-like	Contig16584	**4.42**	**5.67**	**5.17**
	Mucin 5, subtype B	Contig43499	1.12	**−2.02**	**−2.19**
	NLRC like 1	Contig37947	**3.85**	**3.74**	1.13
	NLRC like-10	Contig39985	1.93	2.49	**3.88**
	NLRC like 2	Contig42687	**3.34**	2.28	2.02
	NLRC like 3	Contig31182	1.98	**4.42**	2.24
	NLRC like-4	Contig36542	−1.47	1.83	**2.55**
	NLRC like 5	Contig31317	1.48	**2.71**	2.18
	NLRC like-6	Contig35090	1.46	**3.31**	1.29
	NLRC like-7	Contig14252	4.24	**7.2**	**9.36**
	NLRC like-8	Contig17611	1.75	1.64	**2.68**
	NLRC like-9	Contig29963	2.13	2.31	**2.75**
	NOD-3 like	k_93466446	**2.5**	**2.28**	**2.32**
	Podocan-like (ECMP2-like)	Contig8588	**13.42**	6.6	3.53
	Toll-like receptor 5	Contig14983	1.06	1.51	**2.06**
Endocrine/Growth Disruption	Ghrelin/obestatin preprohormone	Contig41751	**−3.19**	−1.42	1.06
	Igfbp7	Contig7012	**2.24**	−1.02	1.45
	Insulin receptor a	Contig11984	**6.15**	**7.47**	**6.42**
	Insulin-induced gene 1 protein	Contig25801	1.84	−1.77	**−3.08**
	Peptide Y-like	k_83558074	**−5.11**	**−1.52**	**−2.5**
	Relaxin-3	Contig20841	−1.26	−1.52	**−2.92**
	Somatostatin 2-like	k53_727376	**−3.92**	1.2	−2.33

expectation of differing cellular contributions and expression patterns over its length [14]. Clearly, by utilizing pools of the entire length of the intestine, the potential exists for masking or confusing gene expression patterns between differing cellular components or intestinal segments. However, we accepted this compromise in this initial study to more broadly characterize intestinal gene expression. The large number of sequenced contigs and differentially expressed genes captured provided ample numbers of candidates which are likely confined to a single cell type (e.g. mucins, aquaporins), while others such as MHC members and chemokines may be derived from multiple intestinal components. Depending on goals of future research, it may be more appropriate to examine gene expression of these candidates solely in the epithelium (or lamina propria) via laser-capture microdissection or enzymatic

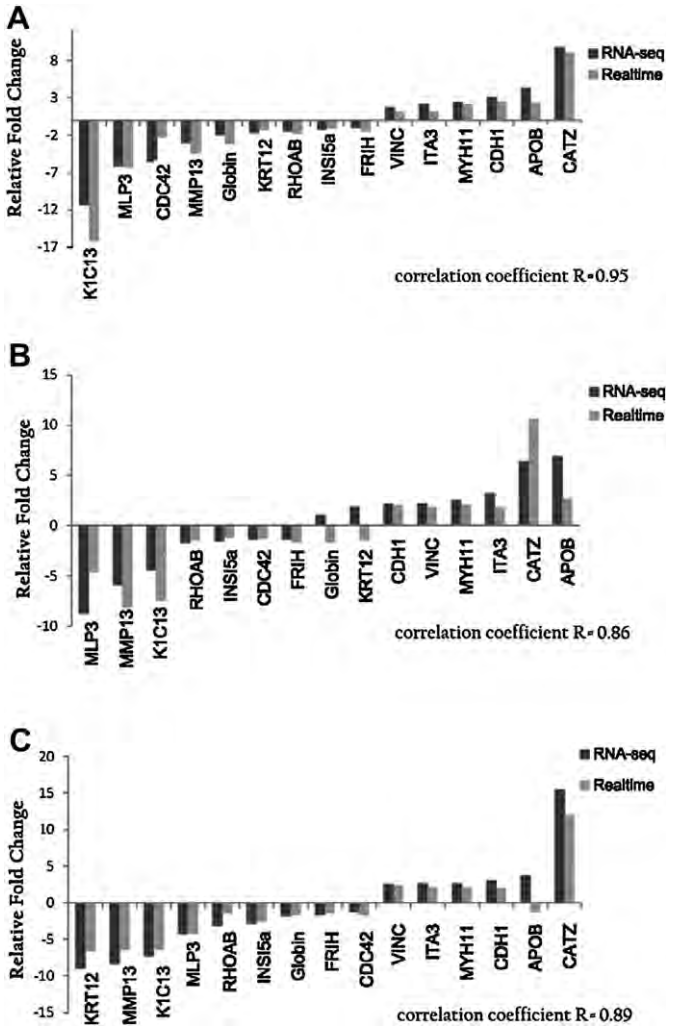

Fig. 2. Comparison of relative fold changes between RNA-seq and QPCR results in catfish intestine gene abbreviations are: Insl5a, Insulin-like 5a; KRT12, Keratin 12; FRIH, Ferritin heavy chain; globin, alpha globin-like; MLP3, myosin light polypeptide 3; APOB, Apolipoprotein B; CDH1, Cadherin 1; VINC, Vinculin; RHOAB, small GTPase RhoA; Integrin, Integrin, ITA3; CATZ, Cathepsin Z; K1C13, Keratin, type I cytoskeletal 13; MMP13, Matrix metalloproteinase 13 preproprotein-like; CDC42, CDC42 small effector protein 2; MYH11, myosin heavy chain 11. A, B, and C represent 3 h, 24 h and 3 d timepoints, respectively. Fold changes are expressed as the ratio of gene expression after *E. ictaluri* challenge to the control group as normalized with 18S rRNA gene.

purification techniques. The time-consuming and expensive nature of these techniques, however, makes it likely that targeted gene assays on large numbers of samples will continue to use whole tissue samples.

Of primary interest in this study was the detection of expression signatures indicative of novel defense strategies and of pathogen-driven manipulation of the cellular machinery of the intestinal epithelium to facilitate entry and replication. We attempted to categorize differentially expressed genes based on six broad functional categories reflective of likely cellular and physiological responses (Table 4). When the identified genes had additional roles outside of or bridging the assigned categories, we attempted to assign functions most appropriate to the context (intestine during infection).

4.1. Cytoskeletal/muscle fiber dynamics

Skirpstunas and Baldwin [21] previously highlighted the potential use of actin polymerization and receptor-mediated endocytosis as modes of infection for *E. ictaluri* in the intestine. Our expression results support their findings with the enrichment of many genes known to play key roles in cytoskeletal rearrangements following infection. The ability of *Salmonella* and *Yersinia*-type bacteria to gain entry through the gut also depends on targeting the actin cytoskeleton [41] and [42] and these bacteria may be excellent models to help inform our understanding of observed molecular changes following *E. ictaluri* infection. Indeed, recent research by Thune et al. [43] indicates that a type III secretion system (T3SS), with functional similarity to that of *Salmonella*, is required for the virulence and replication of *E. ictaluri*. Actin can polymerize into fine and dynamic fibrils or filaments which provide shape and mobility to epithelial cells. Adhesion of bacteria to the host cell surface triggers the accumulation of actin cytoskeletal components forming aggregates and promoting the development of membrane extensions, termed ruffles in the context of *Salmonella* invasion [44]. This bundling of actin filaments facilitates entry via a membrane-containing vacuole that protects the bacteria from lysosomal degradation [3]. Genes associated with bacterially-induced creation of actin-rich structures and observed to be differentially expressed in control and infected catfish intestine included Arp2/3, ezrin, filamin, Rho-GTPase, Cdc42SE2, integrins, gelsolin-like (CAPG), supervillin, AHNAK, and basigin (CD147) among others (Table 4). Gelsolin-like (up-regulated greater than 5-fold at each timepoint) has been observed to be up-regulated in microarray-based studies of *Salmonella* infections in mouse intestine [45] and appears to control membrane ruffling [46]. Some components of actin-rich structures may also serve as receptors or attachment points for pathogens, as in the case of AHNAK, a binding partner for *Chlamydia trachomatis* [47] and up-regulated greater than 7-fold at all timepoints. AHNAK has also been reported to interact with annexin A2 (also differentially expressed in catfish intestine) to regulate cell membrane cytoarchitecture [48]. Another example is basigin, responsible for cell aggregation through cytoskeletal rearrangements, and recently identified as a receptor for *Plasmodium falciparum* [49].

Actomyosin-driven contraction and dynamics can be important in the context of invasion as a central switch controlling both actin polymerization [42] and regulating permeability of apical junctions [50] and [51]. Different myosin components have been reported to be manipulated during pathogen invasion to facilitate entry via endocytosis [42,52]. In *Salmonella* infections, actin and myosin dynamics are manipulated by secreted virulence factors to initially foster entry and then reversed (actin depolymerization) to lead to host cell apoptosis and further spread of the intracellular infection through macrophage uptake [53]. Inflammation, driven by the TNF pathway, may also function to perturb fiber dynamics [54]. Interestingly, actin and myosin genes featured prominently in our differentially expressed gene set (Supplementary Table 2; Table 4), with some patterns likely indicative of up-regulation due to invasion (e.g. Myosin-VII), while others may be indicative of pathogen-induced depolymerization, apoptosis and inflammation (e.g. myosin heavy chain – down-regulated as much as 72-fold; and alpha-actin – down-regulated as much as 21-fold).

4.2. Junctional modification/disruption

Enteric pathogens also often seek to disrupt cellular junctions to gain additional routes of access into the host [3,55]. We observed dysregulation of components of the apical junction complex (AJC), consisting of the tight junction, adherens junction, and desmosome. While permeability-regulating claudins were down-regulated, most other transcripts representing junctional proteins were up-regulated (albeit modestly), including cadherins,

desmoplakin, and MAGI3 among others, potentially as a part of pathogen-induced cytoskeletal rearrangements and binding [56].

4.3. Lysosome/phagosome patterns

A gene signature suggestive of exploitation of the endosomal machinery of catfish for intracellular infection was also detected (Table 4). This included up-regulation of a number of lysosomal surface genes, and differential expression of a number of MHC subunits [41] and several lysosomal acid hydrolases. This latter group, which would be expected to contribute to bacterial killing, was mixed in its expression pattern, with a stronger trend toward down-regulation. NADPH oxidase, and the related NOXO1, responsible for production of reactive oxygen species as part of the intracellular host defense, were both notably down-regulated in the catfish intestine, consistent with reported *Salmonella* evasion strategies [57]. This pattern is particularly notable in the light of the ability of virulent *E. ictaluri* (like *Salmonella*) to survive and replicate within macrophages [58,59]. NADPH oxidase and related genes may serve as potential expression markers for assessing ESC-resistant catfish strains.

4.4. Immune Activation/inflammation

The set of differentially expressed genes encoding innate immune mediators, while large, differed from our initial expectation of a robust up-regulation of defensive strategies and pathways. Indeed, the captured pattern is far more characteristic of immune evasion driven by *E. ictaluri* secreted effectors. We observed dramatic down-regulation (>30-fold at 3 h post infection) of nattectin, a fish C-type lectin, which has been demonstrated to induce the recruitment of specific subsets of monocytes which possess dendritic cell (DC) functions [60]. Interestingly, in one of the few previous studies of intestinal responses to infection in fish, nattectin levels were observed to be higher in disease-resistant gilthead sea bream [16]. CD209 (DC-SIGN), another C-type lectin was also down-regulated, as were MMP13 and MMP9, critical in facilitating migration of DC and monocytes to sites of infection [61]. Indicative of shared mucosal immune responses to fish pathogens, we observed sharp down-regulation of tumor suppressor protein p53 gene at 24 h and 3 d following infection similar to results reported in gills of amoebic gill disease-affected Atlantic salmon [10]. Some innate immune factors known to be up-regulated in response to fish pathogens, were also observed to be down-regulated here, including C1q-like genes [62]; neurotoxin/CD59-like [10,63]; liver-expressed antimicrobial peptide 2 (LEAP-2) [64]; and serum amyloid P [65].

A number of chemokines were differentially expressed following *E. ictaluri* infection. The CC chemokines, highly divergent in fish and extensively characterized by our group previously [23,66,67] were well-represented and showed the largest fold changes at 24 h following infection. CXCL2 and CXCL12, with closer conservation with mammalian counterparts [68], were both up-regulated. Recent research [69,70] indicates that CXCL12 is critical in healing in damaged intestinal epithelium. The pattern of immune evasion continued even among up-regulated genes with macrophage migration inhibitory factor (MIF) and suppressor of cytokine signaling-1 (SOCS1) both induced following bacterial exposure. TNF pathway members, often indicative of harmful inflammation and sepsis, were also up-regulated (Table 4).

4.5. Attachment/pathogen recognition

We separated into a discrete category a number of differentially expressed genes with putative roles in pathogen attachment or host recognition. Among these was an abundance of nucleotide-oligomerization domain (NOD)-like receptor subfamily C (NLRC) genes [71,72] with putative roles in intracellular pathogen recognition. These genes, also referred to as NLRP genes, have dramatically expanded in teleost species [72], often assuming non-canonical domain structures. A subset of the differentially expressed NLRC genes are included in Table 4 (more in Supplementary Table 2), and were observed to be largely up-regulated in contrast to many other immune mediators. Further work is clearly needed to understand the functions and cellular distributions of this diverse group of receptors in fish. Also in this category was TLR5, known to recognize bacterial flagellin, and well-studied in the context of ESC (e.g. [40,73]). Interestingly, in contrast to previous reports of strong up-regulation, we observed only modest up-regulation at 3 d following infection. The lack of a robust TLR5 response may be due to differing sampled tissues (intestine vs. head kidney, spleen, or liver), or may be consistent with a pathogen-suppressed immune response. Russo et al. [74] reported significantly higher TLR5 expression following infection with attenuated *E. ictaluri* relative to expression of TLR5 in fish infected with virulent *E. ictaluri*.

4.6. Endocrine/growth disruption

A final category of interest was composed of differentially expressed genes with putative roles in appetite and growth. Infections in farmed fish are often accompanied by diminished appetite or altered feeding patterns. We observed significant down-regulation of ghrelin, peptide Y-like (PYY), and somatostatin 2-like at 3 h following infection, suggesting that pathogen attachment and entry may rapidly impact important endocrine mediators. In mammals, infection with Gram-negative *Helicobacter pylori* leads to reduced ghrelin concentrations and may be associated with faltering growth [75]. Similarly, decreased concentrations of PYY have been reported in rabbit intestine in response to *Shigella* infections [76]. Future studies should build from these initial observations to study the impact of catfish enteric pathogens and potential therapeutants on neuroendocrine regulation of appetite and growth.

5. Conclusions

Using Illumina RNA-seq technology, we surveyed here for the first time channel catfish transcriptomic responses in the intestine following challenge with the Gram-negative bacterium *E. ictaluri*. The approach was successful in capturing a broad representation of catfish genes (including previously un-sequenced transcripts) and accurately quantifying transcript levels of 1633 differentially expressed genes. The study revealed novel patterns of teleost mucosal gene expression and highlighted unexpected roles for candidate genes and pathways often missed in *a priori* approaches. Utilization of these findings will improve strategies for selection of disease-resistant catfish broodstock and evaluation of prevention and treatment options.

Acknowledgements

This project was supported in part by an Alabama Agriculture Experiment Station Hatch award to E. Peatman under project ALA016-1-09035. Additional support for S. Nandi and S. Mohanty was provided by the Indian Council of Agricultural Research. C. Li was supported by a scholarship from the China Scholarship Council (CSC).

Appendix. Supplementary material

Supplementary material associated with this article can be found, in the online version, at doi:10.1016/j.fsi.2012.02.004.

References

[1] Turner JR. Intestinal mucosal barrier function in health and disease. Nat Rev Immunol 2009;9:799–809.
[2] O'Hara JR, Buret AG. Mechanisms of intestinal tight junctional disruption during infection. Front Biosci 2008;13:7008–21.
[3] Guttman JA, Finlay BB. Tight junctions as targets of infectious agents. Biochim Biophys Acta 2009;1788:832–41.
[4] Niklasson L, Sundh H, Fridell F, Taranger GL, Sundell K. Disturbance of the intestinal mucosal immune system of farmed Atlantic salmon (*Salmo salar*), in response to long-term hypoxic conditions. Fish Shellfish Immunol 2011;31:1072–80.
[5] Perez-Sanchez T, Balcazar JL, Merrifield DL, Carnevali O, Gioacchini G, de Blas I, et al. Expression of immune-related genes in rainbow trout (*Oncorhynchus mykiss*) induced by probiotic bacteria during *Lactococcus garvieae* infection. Fish Shellfish Immunol 2011;31:196–201.
[6] Russell S, Hayes MA, Lumsden JS. Immunohistochemical localization of rainbow trout ladderlectin and intelectin in healthy and infected rainbow trout (*Oncorhynchus mykiss*). Fish Shellfish Immunol 2009;26:154–63.
[7] Komatsu K, Tsutsui S, Hino K, Araki K, Yoshiura Y, Yamamoto A, et al. Expression profiles of cytokines released in intestinal epithelial cells of the rainbow trout, *Oncorhynchus mykiss*, in response to bacterial infection. Dev Comp Immunol 2009;33:499–506.
[8] Bernard D, Six A, Rigottier-Gois L, Messiaen S, Chilmonczyk S, Quillet E, et al. Phenotypic and functional similarity of gut intraepithelial and systemic T cells in a teleost fish. J Immunol 2006;176:3942–9.
[9] Bridle AR, Morrison RN, Nowak BF. The expression of immune-regulatory genes in rainbow trout, *Oncorhynchus mykiss*, during amoebic gill disease (AGD). Fish Shellfish Immunol 2006;20:346–64.
[10] Morrison RN, Cooper GA, Koop BF, Rise ML, Bridle AR, Adams MB, et al. Transcriptome profiling the gills of amoebic gill disease (AGD)-affected Atlantic salmon (*Salmo salar L.*): a role for tumor suppressor p53 in AGD pathogenesis? Physiol Genomics 2006;26:15–34.
[11] Rombout JH, van der Tuin SJ, Yang G, Schopman N, Mroczek A, Hermsen T, et al. Expression of the polymeric Immunoglobulin Receptor (pIgR) in mucosal tissues of common carp (*Cyprinus carpio L.*). Fish Shellfish Immunol 2008;24:620–8.
[12] Rajan B, Fernandes JM, Caipang CM, Kiron V, Rombout JH, Brinchmann MF. Proteome reference map of the skin mucus of Atlantic cod (*Gadus morhua*) revealing immune competent molecules. Fish Shellfish Immunol 2011;31:224–31.
[13] Palaksha KJ, Shin GW, Kim YR, Jung TS. Evaluation of non-specific immune components from the skin mucus of olive flounder (*Paralichthys olivaceus*). Fish Shellfish Immunol 2008;24:479–88.
[14] Rombout JH, Abelli L, Picchietti S, Scapigliati G, Kiron V. Teleost intestinal immunology. Fish Shellfish Immunol 2011;31:616–26.
[15] Jima DD, Shah RN, Orcutt TM, Joshi D, Law JM, Litman GW, et al. Enhanced transcription of complement and coagulation genes in the absence of adaptive immunity. Mol Immunol 2009;46:1505–16.
[16] Davey GC, Calduch-Giner JA, Houeix B, Talbot A, Sitja-Bobadilla A, Prunet P, et al. Molecular profiling of the gilthead sea bream (*Sparus aurata L.*) response to chronic exposure to the myxosporean parasite Enteromyxum leei. Mol Immunol 2011;48:2102–12.
[17] Plumb JA, Chappell J. Susceptibility of blue catfish to channel catfish virus. Proc Annu Conf Southeast Assoc Fish Wildl Agen 1978;32:680–5.
[18] Ourth DD, Chung KT. Purification of antimicrobial factor from granules of channel catfish peripheral blood leucocytes. Biochem Biophys Res Commun 2004;313:28–36.
[19] Griffin BR, Mitchell AJ. Susceptibility of channel catfish, *Ictalurus punctatus* (Rafinesque), to *Edwardsiella ictaluri* challenge following copper sulphate exposure. J Fish Dis 2007;30:581–5.
[20] Hebert P, Ainsworth AJ, Boyd B. Histological enzyme and flow cytometric analysis of channel catfish intestinal tract immune cells. Dev Comp Immunol 2002;26:53–62.
[21] Skirpstunas RT, Baldwin TJ. *Edwardsiella ictaluri* invasion of IEC-6, Henle 407, fathead minnow and channel catfish enteric epithelial cells. Dis Aquat Org 2002;51:161–7.
[22] Peatman E, Terhune J, Baoprasertkul P, Xu P, Nandi S, Wang S, et al. Microarray analysis of gene expression in the blue catfish liver reveals early activation of the MHC class I pathway after infection with Edwardsiella ictaluri. Mol Immunol 2008;45:553–66.
[23] Peatman E, Bao B, Peng X, Baoprasertkul P, Brady Y, Liu Z. Catfish CC chemokines: genomic clustering, duplications, and expression after bacterial infection with Edwardsiella ictaluri. Mol Genet Genomics 2006;275:297–309.
[24] Miller JR, Koren S, Sutton G. Assembly algorithms for next-generation sequencing data. Genomics 2010;95:315–27.
[25] Simpson JT, Wong K, Jackman SD, Schein JE, Jones SJM, Birol I. ABySS: a parallel assembler for short read sequence data. Genome Res 2009;19:1117–23.
[26] Zerbino DR, Birney E. Velvet: algorithms for de novo short read assembly using de Bruijn graphs. Genome Res 2008;18:821–9.
[27] Li W, Godzik A. Cd-hit: a fast program for clustering and comparing large sets of protein or nucleotide sequences. Bioinformatics 2006;22:1658–9.
[28] Huang X, Madan A. CAP3: a DNA sequence assembly program. Genome Res 1999;9:868–77.
[29] Gotz S, Garcia-Gomez JM, Terol J, Williams TD, Nagaraj SH, Nueda MJ, et al. High-throughput functional annotation and data mining with the Blast2GO suite. Nucleic Acids Res 2008;36:3420–35.
[30] Kal AJ, Van Zonneveld AJ, Benes V, Van den Berg M, Koerkamp MG, Albermann K, et al. Dynamics of gene expression revealed by comparison of serial analysis of gene expression transcript profiles from yeast grown on two different carbon sources. Mol Biol Cell 1999;10:1859–72.
[31] Bauer S, Grossmann S, Vingron M, Robinson PN. Ontologizer 2.0-a multifunctional tool for GO term enrichment analysis and data exploration. Bioinformatics 2008;24:1650–1.
[32] Grossmann S, Bauer S, Robinson PN, Vingron M. Improved detection of overrepresentation of Gene-Ontology annotations with parent child analysis. Bioinformatics 2007;23:3024–31.
[33] Pfaffl MW, Horgan GW, Dempfle L. Relative expression software tool (REST) for group-wise comparison and statistical analysis of relative expression results in real-time PCR. Nucleic Acids Res 2002;30:e36.
[34] Martin JA, Wang Z. Next-generation transcriptome assembly. Nat Rev Genet 2011;12:671–82.
[35] Wang S, Peatman E, Abernathy J, Waldbieser G, Lindquist E, Richardson P, et al. Assembly of 500,000 inter-specific catfish expressed sequence tags and large scale gene-associated marker development for whole genome association studies. Genome Biol 2010;11:R8.
[36] Liu S, Zhou Z, Lu J, Sun F, Wang S, Liu H, et al. Generation of genome-scale gene-associated SNPs in catfish for the construction of a high-density SNP array. BMC Genomics 2011;12:53.
[37] Xiang LX, He D, Dong WR, Zhang YW, Shao JZ. Deep sequencing-based transcriptome profiling analysis of bacteria-challenged *Lateolabrax japonicas* reveals insight into the immune-relevant genes in marine fish. BMC Genomics 2010;11:472.
[38] Mu Y, Ding F, Cui P, Ao J, Hu S, Chen X. Transcriptome and expression profiling analysis revealed changes of multiple signaling pathways involved in immunity in the large yellow croaker during *Aeromonas hydrophila* infection. BMC Genomics 2010;11:506.
[39] Li RW, Waldbieser GC. Production and utilization of a high-density oligonucleotide microarray in channel catfish *Ictalurus punctatus*. BMC Genomics 2006;7:134.
[40] Peatman E, Baoprasertkul P, Terhune J, Xu P, Nandi S, Kucuktas H, et al. Expression analysis of the acute phase response in channel catfish (*Ictalurus punctatus*) after infection with a Gram-negative bacterium. Dev Comp Immunol 2007;31:1183–96.
[41] Garcia-del Portillo F, Pucciarelli MG, Jefferies WA, Finlay BB. *Salmonella typhimurium* induces selective aggregation and internalization of host cell surface proteins during invasion of epithelial cells. J Cell Sci 1994;107:2005–20.
[42] Hanisch J, Kolm R, Wozniczka M, Bumann D, Rottner K, Stradal TE. Activation of a RhoA/myosin II-dependent but Arp2/3 complex-independent pathway facilitates *Salmonella* invasion. Cell Host Microbe 2011;9:273–85.
[43] Thune RL, Fernandez DH, Benoit JL, Kelly-Smith M, Rogge ML, Booth NJ, et al. Signature-tagged mutagenesis of *Edwardsiella ictaluri* identifies virulence-related genes, including a salmonella pathogenicity island 2 class of type III secretion systems. Appl Environ Microbiol 2007;73:7934–46.
[44] Hallstrom K, McCormick BA. *Salmonella* interaction with and passage through the intestinal mucosa: through the lens of the organism. Front Microbiol 2011;2:88.
[45] Liu X, Lu R, Xia Y, Sun J. Global analysis of the eukaryotic pathways and networks regulated by *Salmonella typhimurium* in mouse intestinal infection in vivo. BMC Genomics 2010;11:722.
[46] Parikh SS, Litherland SA, Clare-Salzler MJ, Li W, Gulig PA, Southwick FS. CapG(-/-) mice have specific host defense defects that render them more susceptible than CapG(+/+) mice to *Listeria monocytogenes* infection but not to *Salmonella enterica serovar Typhimurium* infection. Infect Immun 2003;71:6582–90.
[47] Hower S, Wolf K, Fields KA. Evidence that CT694 is a novel *Chlamydia trachomatis* T3S substrate capable of functioning during invasion or early cycle development. Mol Microbiol 2009;72:1423–37.
[48] Benaud C, Gentil BJ, Assard N, Court M, Garin J, Delphin C, et al. AHNAK interaction with the annexin 2/S100A10 complex regulates cell membrane cytoarchitecture. J Cell Biol 2004;164:133–44.
[49] Crosnier C, Bustamante LY, Bartholdson SJ, Bei AK, Theron M, Uchikawa M, et al. Basigin is a receptor essential for erythrocyte invasion by. Plasmodium Falciparum Nat 2011;480:534–7.
[50] Turner JR. 'Putting the squeeze' on the tight junction: understanding cytoskeletal regulation. Semin Cell Dev Biol 2000;11:301–8.
[51] Ivanov AI, Bachar M, Babbin BA, Adelstein RS, Nusrat A, Parkos CA. A unique role for nonmuscle myosin heavy chain IIA in regulation of epithelial apical junctions. PLoS ONE 2007;2:e658.

[52] Sousa S, Cabanes D, El-Amraoui A, Petit C, Lecuit M, Cossart P. Unconventional myosin VIIa and vezatin, two proteins crucial for *Listeria* entry into epithelial cells. J Cell Sci 2004;117:2121–30.
[53] Guiney DG, Lesnick M. Targeting of the actin cytoskeleton during infection by *Salmonella* strains. Clin Immunol 2005;114:248–55.
[54] Dekelbab BH, Witchel SF, DeFranco DB. TNF-alpha and glucocorticoid receptor interaction in L6 muscle cells: a cooperative downregulation of myosin heavy chain. Steroids 2007;72:705–12.
[55] Fasano A, Nataro JP. Intestinal epithelial tight junctions as targets for enteric bacteria-derived toxins. Adv Drug Deliv Rev 2004;56:795–807.
[56] Eckmann L, Kagnoff MF. Intestinal mucosal responses to microbial infection. Springer Semin Immunopathol 2005;27:181–96.
[57] Vazquez-Torres A, Xu Y, Jones-Carson J, Holden DW, Lucia SM, Dinauer MC, et al. *Salmonella* pathogenicity island 2-dependent evasion of the phagocyte NADPH oxidase. Science 2000;287:1655–8.
[58] Booth NJ, Beekman JB, Thune RL. *Edwardsiella ictaluri* encodes an acid-activated urease that is required for intracellular replication in channel catfish (*Ictalurus punctatus*) macrophages. Appl Environ Microbiol 2009;75:6712–20.
[59] Russo R, Shoemaker CA, Panangala VS, Klesius PH. In vitro and in vivo interaction of macrophages from vaccinated and non-vaccinated channel catfish (*Ictalurus punctatus*) to Edwardsiella ictaluri. Fish Shellfish Immunol 2009;26:543–52.
[60] Saraiva TC, Grund LZ, Komegae EN, Ramos AD, Conceicao K, Orii NM, et al. Nattectin a fish C-type lectin drives Th1 responses in vivo: licenses macrophages to differentiate into cells exhibiting typical DC function. Int Immunopharmacol 2011;11:1546–56.
[61] Nagase H, Woessner Jr JF. Matrix metalloproteinases. J Biol Chem 1999;274:21491–4.
[62] Carland TM, Locke JB, Nizet V, Gerwick L. Differential expression and intrachromosomal evolution of the sghC1q genes in zebrafish (*Danio rerio*). Dev Comp Immunol 2012;36:31–8.
[63] Martin SA, Blaney SC, Houlihan DF, Secombes CJ. Transcriptome response following administration of a live bacterial vaccine in Atlantic salmon (*Salmo salar*). Mol Immunol 2006;43:1900–11.
[64] Bao B, Peatman E, Xu P, Li P, Zeng H, He C, et al. The catfish liver-expressed antimicrobial peptide 2 (LEAP-2) gene is expressed in a wide range of tissues and developmentally regulated. Mol Immunol 2006;43:367–77.
[65] Huong Giang DT, Van Driessche E, Vandenberghe I, Devreese B, Beeckmans S. Isolation and characterization of SAP and CRP, two pentraxins from Pangasianodon (*Pangasius*) hypophthalmus. Fish Shellfish Immunol 2010;28:743–53.
[66] Bao B, Peatman E, Peng X, Baoprasertkul P, Wang G, Liu Z. Characterization of 23 CC chemokine genes and analysis of their expression in channel catfish (*Ictalurus punctatus*). Dev Comp Immunol 2006;30:783–96.
[67] Peatman E, Liu Z. CC chemokines in zebrafish: evidence for extensive intrachromosomal gene duplications. Genomics 2006;88:381–5.
[68] Baoprasertkul P, He C, Peatman E, Zhang S, Li P, Liu Z. Constitutive expression of three novel catfish CXC chemokines: homeostatic chemokines in teleost fish. Mol Immunol 2005;42:1355–66.
[69] Agle KA, Vongsa RA, Dwinell MB. Calcium mobilization triggered by the chemokine CXCL12 regulates migration in wounded intestinal epithelial monolayers. J Biol Chem 2010;285:16066–75.
[70] Agle KA, Vongsa RA, Dwinell MB. Chemokine stimulation promotes enterocyte migration through laminin-specific integrins. Am J Physiol Gastrointest Liver Physiol 2011;301:G968–80.
[71] Sha Z, Abernathy JW, Wang S, Li P, Kucuktas H, Liu H, et al. NOD-like subfamily of the nucleotide-binding domain and leucine-rich repeat containing family receptors and their expression in channel catfish. Dev Comp Immunol 2009;33:1–999.
[72] Hansen JD, Vojtech LN, Laing KJ. Sensing disease and danger: a survey of vertebrate PRRs and their origins. Dev Comp Immunol 2011;35:886–97.
[73] Bilodeau AL, Waldbieser GC. Activation of TLR3 and TLR5 in channel catfish exposed to virulent *Edwardsiella ictaluri*. Dev Comp Immunol 2005;29:713–21.
[74] Russo R. An Attenuated Strain of *Edwardsiella ictaluri* is killed by channel catfish (*Ictalurus punctatus*) macrophages and confers protection in few days. Dyn Biochem Process Biotech Mol Biol; 2011:76–82.
[75] Osawa H, Nakazato M, Date Y, Kita H, Ohnishi H, Ueno H, et al. Impaired production of gastric ghrelin in chronic gastritis associated with Helicobacter pylori. J Clin Endocrinol Metab 2005;90:10–6.
[76] Svensson L, Bergquist J, Wenneras C. Neuromodulation of experimental *Shigella* infection reduces damage to the gut mucosa. Microbes Infect 2004;6:256–64.